Inorg. Chem. **2003**, *42*, 6345–6351

$Cr[(H_3N–(CH_2)_2–PO_3)(Cl)(H_2O)]$: X-Ray Single-Crystal Structure and Magnetism of a Polar Organic–Inorganic Hybrid Chromium(II) Organophosphonate

Elvira M. Bauer,[†] Carlo Bellitto,*[,†] Marcello Colapietro,*[,‡] Gustavo Portalone,[‡] and Guido Righini[†]

Istituto di Struttura della Materia—CNR Sez. Montelibretti, via Salaria km 29.300, P.O. Box 10, I-00016 Monterotondo Staz. (RM), Italy, and Department of Chemistry, University of Rome "La Sapienza", P. le A. Moro, 5, I-00185 Roma, Italy

Received March 26, 2003

$Cr[(H_3N–(CH_2)_2–PO_3)(Cl)(H_2O)]$, a rare example of a polar organic–inorganic hybrid material containing Cr^{2+}, was prepared from $CrCl_2$, 2-aminoethylphosphonic acid, and urea in water and isolated as light-blue crystals. It crystallizes in the noncentrosymmetric monoclinic space group $P2_1$, with $a = 5.249(1)$ Å, $b = 14.133(3)$ Å, $c = 5.275(1)$ Å, and $\beta = 105.55(2)°$. The inorganic layer of the hybrid network is formed by Cr(II) five-coordinated by three oxygen atoms from the phosphonates and one from the water molecule in a square pyramidal unit, whose apical position is occupied by the Cl^- ion. Hydrogen bonds are established between the coordinating water molecule and the oxygen atoms of adjacent phosphonate ligands. The inorganic network is interspersed by ethylammonium groups, and the terminal ammonium moiety is linked to the apical Cl^- ions through hydrogen bonds. Electrostatic interactions as well as hydrogen bonds and the coordinated chlorine atoms ensure the cohesion of the 3D structure. The lattice is polar (lack of inversion center), and this fact determines the magnetic behavior of the compound at low temperatures. The magnetic susceptibility data in the temperature range from 300 to 50 K show Curie–Weiss behavior, with $C = 2.716$ cm^3 K mol^{-1} and the Weiss constant $\theta = -2.2$ K. The corresponding effective magnetic moment of 4.7 μ_B compares well with the expected value for Cr^{2+} in d^4 high-spin configuration. A slight decrease of the χT product versus T observed at temperatures below 50 K indicates nearest-neighbor antiferromagnetic exchange interactions. On cooling below $T = 6$ K, the magnetic susceptibility increases sharply up to a maximum at ca. 5 K and then decreases again. Below $T = 6$ K, hysteresis loops taken at different temperatures show that $Cr[(H_3N–(CH_2)_2–PO_3)(Cl)(H_2O)]$ behaves as a weak ferromagnet with the critical temperature T_N at 5.5 K. The spin canting is responsible of the long-range magnetic ordering. The values of the coercive field, H_c, and of remnant magnetization, M_r, obtained from the hysteresis loop at $T = 4.5$ K (the lowest measured temperature) are 30 Oe and 0.08 μ_B, respectively.

Introduction

Metal(II) phosphonates $M^{II}[RPO_3(H_2O)]$, where M is a divalent first series transition metal ion and R is an organic group, have provided interesting examples of magnetic solids.[1,2] They crystallize often in a lamellar structure, with alternating organic and inorganic layers along one direction of the unit-cell.[3] The inorganic layers consist of metal ions bridged by the oxygen atoms of phosphonate groups, and the resulting metal−oxygen network forms sheets that are separated one from the other by the organic R-group of the ligand. These materials belong to a wide class of compounds known as hybrid organic−inorganic composites.[4] They offer

* To whom correspondence should be addressed. E-mail: Carlo.Bellitto@ism.cnr.it (C.B.); m.colapietro@caspur.it (M.C.). Phone: ++39 06 90672319 (C.B.); ++39 06 49913715 (M.C.). Fax: ++39 06 90672316 (C.B.).
† Istituto di Struttura della Materia—CNR Sez. Montelibretti.
‡ Department of Chemistry, University of Rome "La Sapienza".

(1) See for example: (a) Bellitto, C. In *Magnetism: Molecules to Materials*; Miller, J. S., Drillon M., Eds.; Wiley-VCH: Weiheim, 2001; Vol. 2, pp 425−456. (b) Mingotaud, C.; Delhaes, P.; Meisel, M. W.; Talham, D. R. In *Magnetism: Molecules to Materials*; Miller, J. S., Drillon M., Eds.; Wiley-VCH: Weiheim, 2001; Vol. 2, pp 457−484.
(2) Gutschke, S. O. H.; Price, D. R.; Powell, A. K.; Wood, P. T. *Angew. Chem., Int. Ed.* **1999**, *38*, 1088.
(3) (a) Alberti, G. In *Comprehensive Supramolecular Chemistry*; Lehn, J. M., Ed.; Pergamon Press: Oxford, 1996; Vol. 7, pp 151−185. (b) Clearfield, A. *Prog. Inorg. Chem.* **1998**, *47*, 371.
(4) Mitzi, D. B. *Prog. Inorg. Chem.* **1999**, *48*, 1.

10.1021/ic0343197 CCC: $25.00
Published on Web 09/09/2003

the possibility of integrating useful organic and inorganic characteristics within a single crystalline molecular-scale composite, forming unique electronic, optical, and magnetic properties. The organic part of the phosphonic acid, $[RPO_3]^{2-}$, can be chemically modified by introducing another donor group, such as the hydroxy group, the amino group, or even another phosphonate group. The two centers of coordination then may induce self-assembling with the possible formation of a 3D hybrid structure[4] bound covalently and/or ionically. Now, if the metal ions contain unpaired spins, the compound at low temperatures can feature magnetic properties typical of low-dimensional magnetic solids and possibly 3D long-range magnetic ordering. In the case of $M^{II}[C_nH_{2n+1}PO_3\cdot(H_2O)]$ ($n = 1-18$; M(II) = Mn, Fe, Ni), a long-range antiferromagnetic order at low temperatures has been observed,[5,6] and more significantly, below the critical temperature, T_N, they are canted antiferromagnets or weak ferromagnets.[7] In addition, only the bis-hydrate form of the nickel(II) methylenediphosphonate shows a ferromagnetic long-range order at $T_C = 3.8$ K.[8] Furthermore, a few years ago several interesting magnetic Cr(II) organophosphonates were isolated by our group, but the polycrystalline nature of the solids has prevented the study of their crystal structures.[9] In an attempt to obtain information on the crystal structure and possibly study the correlation between the crystal structures of some Cr(II) phosphonates and their magnetic properties, we have grown single crystals of $Cr[(H_3N-(CH_2)_2-PO_3)(Cl)(H_2O)]$.

In the present contribution, we wish to report on the first X-ray single-crystal study of a polar (noncentrosymmetric) magnetic Cr(II) ammonium−ethylphosphonate−chloride: i.e., $Cr[(H_3N-(CH_2)_2-PO_3)(Cl)(H_2O)]$. The formation of crystals having a polar axis is regarded as one of the most remarkable aspects of the solid-state chemistry. Polar molecular materials may in fact show some interesting phenomena, such as pyroelectric, ferroelectric, or piezoelectric effects or even the nonlinear optical effect (second harmonic generation, SGH), and all of them are already of enormous technological importance.[10] These molecule-based compounds can also provide examples of multiproperty materials, if they are, for example, magnetic.[11]

Experimental Section

Reagents were of analytical grade and used without further purification. All reactions involving the Cr(II) ion were carried out under inert atmosphere working with the Schlenk techniques. HPLC water (Carlo Erba) was used as a solvent and purged previously with N_2 gas.

Synthesis of $Cr[(H_3N-(CH_2)_2-PO_3)(Cl)(H_2O)]$. $CrCl_2$ (3.26 g, 26.5 mmol) was dissolved in water (10 mL), filtered, and added to a colorless mixture containing water, 2-aminoethyl phosphonic acid (3.31 g, 26.5 mmol), and urea (3.18 g, 53 mmol). The resulting blue solution was heated under nitrogen at $T = 80$ °C. After a few days, a blue microcrystalline solid was separated by filtration, washed with water and methanol, and dried under vacuum at room temperature. The compound decomposes after several days of exposure to the air, depending on the size of the crystallites. UV−vis (diffuse reflectance, nm): 230 (s), 440 (sh), 680 (s, br), 840 (sh). Anal. Calcd for $Cr[(H_3N-(CH_2)_2-PO_3)(Cl)(H_2O)]$, $C_2H_9NClCrO_4P$: C, 10.47; H, 3.95; N, 6.10; Cl, 15.45; Cr, 22.65; P, 13.49. Found: C, 10.48; H, 3.97; N, 6.09; Cl, 15.42; Cr, 22.54; P, 13.68.

Elemental analysis was performed by the Malissa & Reuter Laboratory, Elbach, Germany. Thermogravimetric analysis data were collected in flowing dry N_2 gas at the rate of 5 °C/min on a Stanton-Redcroft STA-781 thermoanalyzer. The IR absorption spectra were obtained by using a Perkin-Elmer 621 spectrophotometer by the KBr method. UV−vis diffuse reflectance spectra were recorded on a Varian Cary 5E equipped with a diffuse reflectance sphere. Static magnetic susceptibility and magnetization measurements were performed by using a Quantum Design MPMS5 SQUID susceptometer in fields up to 5 T from 300 to 4.2 K. The susceptibility measurements as a function of temperature below $T = 4.2$ K were performed with a SQUID Quantum Design MPMS7 by Dr. M. Green at the Royal Institution of Great Britain, London. A cellulose capsule was filled with a freshly prepared polycrystalline sample and placed inside a polyethylene straw. All the experimental data were corrected for the core magnetization using Pascal's constants ($\chi_d = 1.362 \times 10^{-4}$ cm^3 mol^{-1}).

X-ray Crystallography. X-ray Powder Diffraction Studies. Room-temperature X-ray powder diffraction data were collected on a Seifert XRD-3000 diffractometer equipped with a curved graphite single-crystal monochromator [$\lambda(K\alpha_1, K\alpha_2) = 1.5406/1.5444$ Å] and a scintillation detector. Data were collected with a step size of 0.02°, 2θ, and at count time of 4 s per step of 0.2° min^{-1} over the range $4° < 2\theta < 80°$. The sample was mounted on a glass flat plate, giving rising to a strong preferred orientation. The diffractometer zero point was determined from an external Si standard.

X-ray Single-Crystal Studies. The crystal used for the X-ray diffraction studies was a light-blue platelet of dimensions $0.10 \times 0.10 \times 0.20$ mm^3. Details of the crystal data, data collection, structure solution, and refinement are reported in Table 1. Data were collected on a Huber CS diffractometer,[12] with graphite monochromatized Mo Kα radiation ($\lambda = 0.71069$ Å), using ω-scan. The crystal used for diffraction studies showed no decomposition during data collection. The data were corrected for Lp and for absorption, and the structure was solved by direct methods and refined by least-squares method using the SIR-CAOS package.[13a,b] The hydrogen atoms of the water molecule were not unambiguously located through a Fourier synthesis and consequently not introduced into the final least-squares refinement. The remaining hydrogen

(5) (a) Carling, S. G.; Day, P.; Visser, D.; Kremer, R. K. J. *Solid State Chem.* **1993**, *106*, 111. (b) Fanucci, G. E.; Krzystek, J.; Meisel, M. W.; Brunel, L.-C.; Talham, D. R. *J. Am. Chem. Soc*. **1998**, *120*, 5469.
(6) (a) Bellitto, C.; Federici, F.; Ibrahim, S. A.; Mahmoud, M. R. *1998 MRS Fall Meetings Proceedings*, Boston, MA, 1999; Vol. 547, p 487. (b) Altomare, A.; Bellitto, C.; Ibrahim, S. A.; Mahmoud, R. F.; Rizzi, R. *J. Chem. Soc., Dalton Trans.* **2000**, 3913. (c) Altomare, A.; Bellitto, C.; Ibrahim, S. A.; Rizzi, R. *Inorg. Chem.* **2000**, *39*, 1803. (d) Bellitto, C.; Colapietro, M.; Caschera, D.; Federici, F.; Portalone, G. *Inorg. Chem.* **2002**, *41*, 709. (e) Bellitto, C.; Bauer, E. M.; Ibrahim, S. A.; Mahmoud, R. F.; Righini, G. *Chem. Eur. J.* **2003**, *6*, 1324.
(7) See for example: (a) Carlin, R. L. *Magnetochemistry*; Springer-Verlag: Berlin, 1986; pp 148−154. (b) Moriya, T. *Phys. Rev.* **1960**, *117*, 635. (c) Dzyaloshinsky, I. *J. Phys. Chem. Solids* **1958**, *4*, 241.
(8) Gao, Q.; Guillou, N.; Nogue, M.; Cheetham, A. K.; Ferey, G. *Chem. Mater*. **1999**, *11*, 2937.
(9) (a) Bellitto, C.; Federici, F.; Ibrahim, S. A. *J. Chem. Soc., Chem. Commun*. **1996**, 759. (b) Bellitto, C.; Federici, F.; Ibrahim, S. A. *Chem. Mater*. **1998**, *10*, 1076.
(10) Curtin, D. Y.; Paul, I. C. *Chem. Rev*. **1981**, *81*, 525.
(11) (a) Rabu, P.; Drillon, M. *Adv. Eng. Mater*. **2003**, *5*, 189. (b) Lacroix, P. G.; Malfant, I.; Bernard, S.; Yu, P.; Riviere, E.; Nakatani, K. *Chem. Mater*. **2001**, *13*, 441.
(12) Colapietro, M.; Cappuccio, G.; Marciante, C.; Pifferi, A.; Spagna, R.; Helliwell, J. R. *J. Appl. Crystallogr.* **1992**, *25*, 192.

Table 1. Crystallographic Data for $Cr[(H_3N(CH_2)_2PO_3)(Cl)(H_2O)]$

Crystal Data	
empirical formula	$C_2H_9ClCrNO_4P$
habit, color	plates, light-blue
crystal size (mm^3)	$0.10 \times 0.10 \times 0.20$
fw	229.52
cryst syst	monoclinic
space group	$P2_1$
a (Å)	5.249(1)
b (Å)	14.133(3)
c (Å)	5.275(1)
β (deg)	105.55(2)
V ($Å^3$)	377.0(1)
Z	2
ρ_{calcd} (g cm^{-3})	2.022
T (K)	293
radiation (Å)	Mo Kα ($\lambda = 0.71069$)
2θ range (deg)	4−60
h, k, l collected	±7, 0−16, ±7
μ (mm^{-1})	2.040
reflns collected	7106
unique reflns with $\|F_o\| \geq 3\sigma\|F_o\|$	1523
Structure Solution and Refinement	
refinement	$\|F_o\|$
solution method	direct methods
quantity minimized	$\sum w(F_o - F_c)^2$
weighting scheme	$1/(0.11240 + 0.00202\|F_o\| + 0.00062\|F_o\|^2)$
no. params refined	91
$R(F)^a$	0.0241
$R_w(F)^b$	0.0346
R_{int}	0.0210
GOF	0.840

$^a R(F) = \sum(|F_o| - |F_c|)/\sum|F_o|$. $^b R_w(F) = \sum w(|F_o| - |F_c|)^2/\sum w|F_o|^2$.

atoms belonging to the methylene and $-NH_3^+$ moieties were introduced in idealized positions (C−H, N−H = 0.96 Å) with fixed isotropic temperature factors, and a riding model was used in the final refinement. The residual electron density is in the range −0.47(8) to 0.47(8) e $Å^{-3}$. All final calculations were done with PARST package,[13c] and molecular graphics were obtained with ORTEP-3 package.[13d]

Results

The title compound was isolated as a light-blue microcrystalline solid from the reaction of 2-aminoethylphosphonic acid and $CrCl_2$ in water, and besides, single crystals were also grown successfully. $Cr[(H_3N-(CH_2)_2-PO_3)(Cl)(H_2O)]$ contains an organic ammonium group. The protonation of the amino group in metal phosphonate derivatives was previously observed only in $Zr[H_3N-(CH_2)_2-PO_3]_2(Cl)_2$,[14] but no crystal structure of the latter was reported. TGA and DSC studies confirmed the presence of coordinated water in the material. Upon heating, $Cr[(H_3N-(CH_2)_2-PO_3)(Cl)(H_2O)]$ is stable up to ~230 °C. In the temperature range from 230 to 300 °C, the material loses 8.5% of the initial weight, and at even higher temperatures, up to 427 °C, a second mass loss occurs which is 9.7% in weight. These mass losses agree with the removal of one water molecule and ammonia per formula unit (total mass loss calculated: 15.22%). At higher temperatures a third weight loss corresponding to the decomposition of the organic part of the ligand can be observed.

Table 2. Selected Bond Lengths (Å) and Angles (deg) for Non-Hydrogen Atoms for $Cr[(H_3N(CH_2)PO_3)(Cl)(H_2O)]$ with esd's in Parentheses as Units on the Last Digit

Cr−O_1	1.995(2)	P−O_2	1.537(2)
Cr−O_2	2.024(2)	P−O_3	1.522(2)
Cr−O_3	2.012(2)	P−C_1	1.805(3)
Cr−O_4	2.041(2)	C_1−C_2	1.518(4)
Cr−Cl	2.730(2)	C_2−N	1.487(4)
P−O_1	1.515(2)		
Cr−O_3−P	153.0(2)	O_3−Cr−O_4	175.5(1)
O_1−P−O_2	108.2(1)	O_1−P−O_3	114.0(1)
O_2−P−O_3	111.5(1)	Cl−Cr−O_1	96.1(1)
Cl−Cr−O_2	94.6(1)	Cl−Cr−O_3	91.0(1)
Cl−Cr−O_4	89.5(1)		

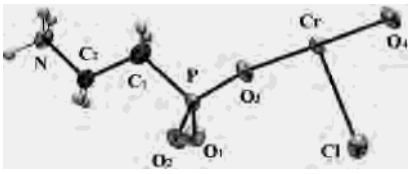

Figure 1. Schematic representation of the $Cr[(H_3N(CH_2)_2PO_3)(Cl)(H_2O)]$ molecule, showing the asymmetric unit and the numbering scheme. Thermal ellipsoids are drawn at 50% probability level.

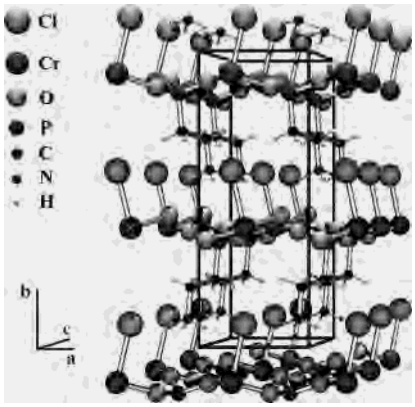

Figure 2. Unit-cell packing of $Cr[(H_3N(CH_2)_2PO_3)(Cl)(H_2O)]$ viewed along the c-axis. The Cr−Cl axis is almost parallel to the b-axis.

Crystal and Molecular Structure of $Cr[(H_3N-(CH_2)_2-PO_3)(Cl)(H_2O)]$. $Cr[(H_3N-(CH_2)_2-PO_3)(Cl)(H_2O)]$ crystallizes in the noncentrosymmetric monoclinic space group $P2_1$ with the following unit-cell parameters: $a = 5.249(1)$ Å, $b = 14.133(3)$ Å, $c = 5.275(1)$ Å, $\beta = 105.55(2)°$, $V = 377.0(1)$ $Å^3$; $Z = 2$; $\rho_{calcd} = 2.022$ g cm^{-3}, $T = 293$ K. Atomic positional and thermal parameters of the asymmetric unit are included in the Supporting Information. Selected bond lengths and bond angles are given in Table 2. The asymmetric unit of the title compound with the numbering scheme used in the tables is shown in Figure 1. The unit-cell packing along the c-axis and b-axis is reported in Figures 2 and 3, respectively. The compound is lamellar and consists of alternating inorganic and organic layers. The most relevant feature of the complex is that it crystallizes in the noncentrosymmetric space group $P2_1$, with all the molecules almost parallel to the b-axis (polar crystal axis) of the unit-cell, and all the chlorine atoms pointing in the same direction. The inorganic layers are made of square-pyramidal Cr^{II} chro-

(13) (a) Altomare, A.; Burla, M. C.; Camalli, M.; Cascarano, G.; Giacovazzo, C.; Guagliardi, A.; Moliterni, A. G.; Polidori, G.; Spagna, R. *J. Appl. Crystallogr.* **1999**, *32*, 115. (b) Camalli, M.; Spagna, R. *J. Appl. Crystallogr.* **1994**, *27*, 861. (c) Nardelli, M. *Comput. Chem.* **1983**, *7*, 95. (d) Farrugia, L. J. *J. Appl. Crystallogr.* **1997**, *30*, 565.
(14) Casciola, M.; Costantino, U.; Peraio, A.; Rega, T. *Solid State Ionics* **1995**, *77*, 229.

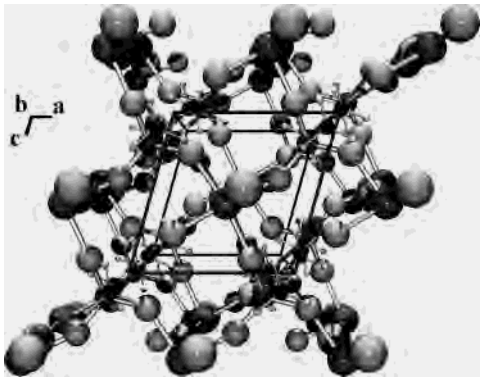

Figure 3. Unit-cell packing of $Cr[(H_3N(CH_2)_2PO_3)(Cl)(H_2O)]$ viewed along the *b*-axis.

mophores, [CrO_4 + 1Cl], coordinated in the basal plane by three oxygen atoms of three different phosphonates and by one oxygen atom (O4) of the water molecule, thus forming an almost square planar [CrO_4] unit. The fifth apical position is occupied by the Cl^- anion. The four Cr−O bond lengths in the square-planar arrangement are close to the distances found in other pentacoordinated Cr(II) compounds based on [CrO_5] units.[15] The Cr−Cl bond distance (i.e., 2.73(2) Å) is slightly longer than that observed in the octahedral [$CrCl_6$] chromophore of the compound $(C_nH_{2n+1}NH_3)_2CrCl_4$[16] but similar to the apical Cr−Cl bond observed in the square-pyramidal [CrO_4Cl] polyhedra of $Cr_4(Si_2O_7)Cl_2$[17] (i.e., 2.694 Å), confirming the tendency of the axial halide ligand to prefer longer (weaker) bonds.

As a result of this coordination, adjacent square-pyramids are connected by two oxygens (O_1 and O_3 or O_2 and O_3) of the same phosphonate ligand to form cross-linked zigzag chains in the (*ac*) plane. The square-pyramid is distorted and tilted by 16.4(1)° with respect to the *b*-axis. The O−Cr−O bond angles range between 85.5(1)° and 97.1(1)°, and the Cr atom lies 0.098(1) Å from the basal plane [CrO_4]. The angle between the mean square plane defined by the oxygens of the [CrO_4] unit and the Cr−Cl bond is 89.2(1)°. The symmetry of the $[-PO_3]^{2-}$ group is not C_{3v} but lower, with the three O−P−O angles significantly different ($O_1-P_1-O_2$ = 108.2(1)°, $O_1-P_1-O_3$ = 114.0(1)°, $O_2-P_1-O_3$ = 111.5(1)°). Another remarkable feature of this structure is represented by the hydrogen bonds established between the coordinated water molecule and the oxygens of adjacent ligands. The inorganic layers are held together by ethylammonium groups; i.e., the terminal ammonium group is located in the cavity formed by adjacent apical chloride ligands, and hydrogen bonds are also established between them (see below). The tilting of the [CrO_4 + 1Cl] square-pyramids alternates along the *b*-axis. On the whole, the layered hybrid system is composed of covalent inorganic [CrO_4 + 1Cl] layers, alternating with the organic ones, which are ionically bonded to the adjacent layers and oriented toward the

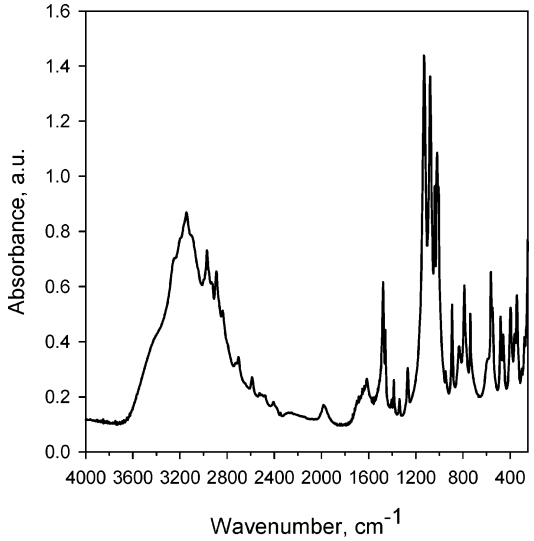

Figure 4. IR spectrum of $Cr[(H_3N(CH_2)_2PO_3)(Cl)(H_2O)]$ in the KBr region.

($-NH_3^+$) groups. All these types of bonds are responsible of the cohesion of the crystal lattice, and this explains the thermal stability and the slow decomposition in air of the title compound.

The presence of the single phase in the microcrystalline powder used for the magnetic measurements was ascertained by the Rietveld[18] analysis of X-ray powder diffraction data by using as a model the structure of the single crystal.

Optical Properties. The FTIR spectrum of $Cr[(H_3N(CH_2)_2PO_3)(Cl)(H_2O)]$ is reported in Figure 4. It features a broad absorption in the region 3500−2500 cm^{-1}, assigned to the stretching of the NH_3^+ group superimposed by the O−H stretching of coordinated water. Nevertheless, comparison with other Cr(II) alkyl phosphonates[9b] permits us to identify the large shoulder centered at ∼3246 cm^{-1} as O−H stretching of coordinated water while the asymmetric and symmetric stretching modes of the amino group are located at lower energies, i.e., 3200−2500 cm^{-1}, thus indicating that the amino group of the ligand is protonated.[19] The corresponding asymmetric deformation mode of the ($-NH_3^+$) group can be identified as a shoulder at 1680 cm^{-1}, and the absorption due to the O−H bending mode is located at 1610 cm^{-1}. Asymmetric and symmetric C−H stretching vibrations of the two methylene fragments bonded to two different functional groups, i.e., ($-NH_3^+$) and $[PO_3]^{2-}$, give rise to several bands of medium intensity in the range 2972−2836 cm^{-1}.[20] Vibrations of medium to weak intensity in the range 1400−1200 cm^{-1} are due to the CH_2 deformation and wagging modes. Five very strong bands are observed at 1130, 1078, 1040, 1018, and 1008 cm^{-1}, respectively. They are

(15) (a) Maass K.; Glaum, R. *Acta Crystallogr.* **2000**, *C56*, 404. (b) Stock, N.; Férey, G.; Cheetham, A. K. *Solid State Sci.* **2000**, *2*, 307.
(16) Babar, M. A.; Ladd, M. F. C.; Larkworthy, L. F.; Povey, D. C.; Proctor, K. J.; Summers, L. J. *J. Chem. Soc., Chem. Commun.* **1981**, 1046.
(17) Schmidt, A.; Glaum, R.; Beck, J. *J. Solid State Chem.* **1996**, *127*, 331.
(18) (a) Rietveld, H. M. *J. Appl. Crystallogr.* **1969**, *2*, 65. (b) Larson, A. C.; Von Dreele, R. B. *GSAS: Generalized Structure Analysis System*; Report LAUR 86-748; Los Alamos National Laboratory: Los Alamos, NM, 1994.
(19) (a) Fenot, P.; Darriet, J.; Garrigou-Lagrange, C.; Cassaigne, A. *J. Mol. Struct.* **1978**, *43*, 49. (b) Rosenthal, G. L.; Caruso, J. *Inorg. Chem.* **1992**, *31*, 3104. (c) Drumel, S.; Janvier, P.; Barboux, P.; Bujoli-Doueff, M.; Bujoli, B. *Inorg. Chem.* **1995**, *34*, 148.
(20) Socrates, G. *Infrared and Raman Characteristic Group Frequencies*; J. Wiley & Sons: Chichester, U.K., 2001.

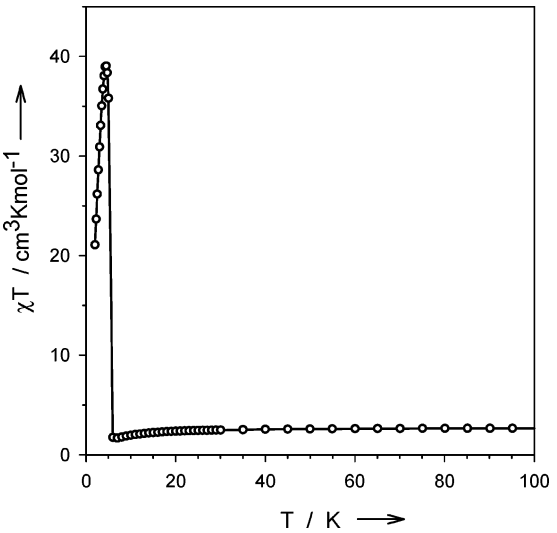

Figure 5. χT vs T plots of $Cr[(H_3N(CH_2)_2PO_3)(Cl)(H_2O)]$ in the temperature range 2−100 K measured at an applied field of 100 Oe.

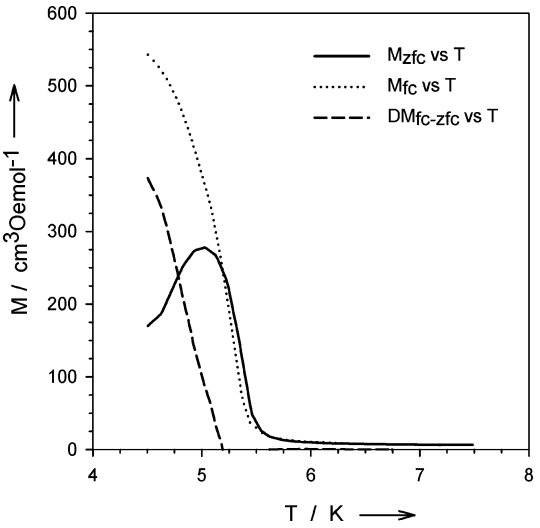

Figure 6. Temperature dependence of the zfc (—) and fc (···) magnetization of $Cr[(H_3N(CH_2)_2PO_3)(Cl)(H_2O)]$ below 10 K at an applied field of 25 Oe. The dotted line ΔM_{fc-zfc} (- - -) represents the difference between the fc and zfc magnetizations.

characteristic for the very strong P−O stretches, the rotation vibrations of the NH_3^+ fragment, and a prominent visible C−N stretching mode.[19a]

The diffuse reflectance electronic spectrum of $Cr[(H_3N(CH_2)_2PO_3)(Cl)(H_2O)]$ displays a broad band at 14700 cm^{-1} together with a shoulder at the lower energy side (∼11900 cm^{-1}). This absorption can be assigned to the d−d transitions of pentacoordinated Cr(II) on the basis of the crystal spectra studies undertaken on a similar isoelectronic $MnCl_5$ complex, i.e., $[(C_2H_4)_4N]_2Mn(III)Cl_5]$.[21] A second broad band of low intensity has been found at 22700 cm^{-1}. The position and intensity of this band are sufficient to consider a charge-transfer transition in this region of the electronic spectra. At least a very strong absorption, which has been observed at high energies (43400 cm^{-1}), is probably due to the $\pi-\pi^*$ bands of the ethylammonium ligand.

Magnetic Properties. $Cr[(H_3N(CH_2)_2PO_3)(Cl)\cdot H_2O]$ is a typical paramagnetic system in the temperature range 30−300 K. It obeys the Curie−Weiss law, the Curie constant, C, being 2.716 cm^3 K mol^{-1}, and the value of the Weiss constant, $\theta = -2.2$ K. The corresponding effective magnetic moment of 4.7 μ_B is consistent with the presence of a Cr^{II} ion in the d^4 ($S = 2$) high-spin configuration (spin-only value 4.9 μ_B). In the temperature range 50−6 K, a slight decrease of the product χT is observed, thus indicating antiferromagnetic nearest-neighbor exchange interactions in accordance with the small negative value of θ (see Figure 5). Interestingly, a sharp increase of the product χT is observed below $T = 5.7$ K, and a maximum of ≅ 40 cm^3 K mol^{-1} (for an applied field of 100 Oe) at $T \cong 5$ K is reached. This abrupt increase of χT in the low-temperature region can be attributed to the spin canting.[7] Field-cooled magnetization (M_{fc}) and the zero-field-cooled (M_{zfc}) magnetization plots, measured in the temperature range 4.2−10 K at the applied field of 25 G, are reported in Figure 6. The two plots do not overlap and reveal the occurrence of magnetic ordering below $T =$ 6 K. The M_{fc} versus T plot shows a rapid increase at $T =$ 5.7 K, while the M_{zfc} versus T plot shows a narrow peak with the maximum at $T_{max} \sim 5$ K. The difference between M_{fc} and M_{zfc} plots represents the spontaneous magnetization, ΔM_{fc-zfc}, induced on cooling below the critical temperature within that field and after switching off the field. The ΔM_{fc-zfc} versus T plot drops to zero at $T \cong 5.5$ K. With the aim of locating the temperature at which the ordered magnetic state appears, several hysteresis loops between 4.5 and 6.0 K were recorded. The hysteresis loop M versus H, measured at $T = 4.5$ K (the lowest measured temperature) shows an S shape typical for a weak ferromagnet[7a] (see Figure 7), and the magnetization $M(H,T)$ is given by two contributions:

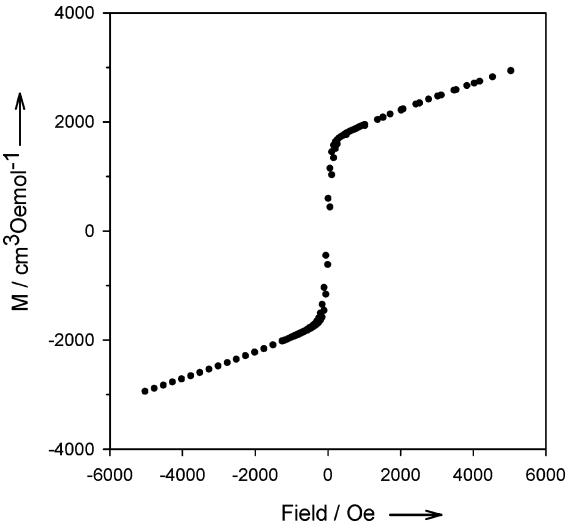

Figure 7. Hysteresis loop at $T = 4.5$ K.

$$M(H,T) = M_{nc}(H,T) + \chi_{AFM}(T)\cdot H$$

where $M_{nc}(T)$ is the uncompensated (weak ferromagnetic) moment and χ_{AFM} is the antiferromagnetic susceptibility. $M_{nc}(T)$ was determined from extrapolation to zero-field of

(21) Bellitto, C.; Tomlinson, A. A. G.; Furlani, C. *J. Chem. Soc. A* **1971**, 3267.

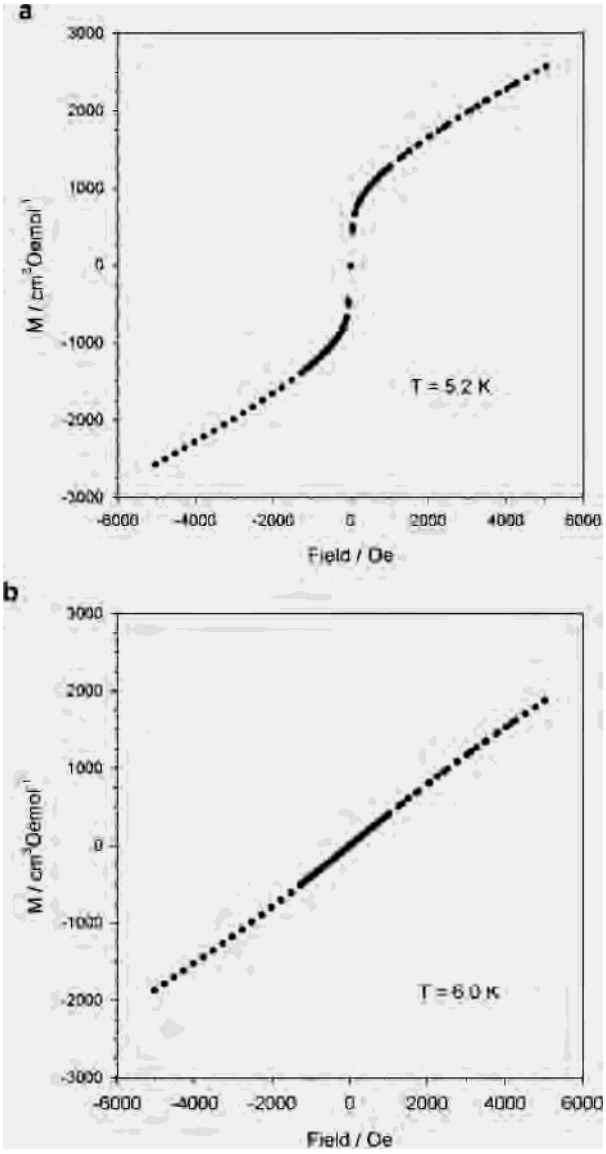

Figure 8. Hysteresis loops at $T = 5.2$ K (a) and at $T = 6.0$ K (b).

the linear part of the magnetization curve at high applied magnetic fields. At $T = 4.5$ K, the coercive field, H_c, and a remnant magnetization, M_{nc}, were found to be 30 Oe and 1785 cm^3 Oe mol^{-1}, respectively. The value of M_{nc} (4.5 K) represents a small fraction of the value expected for a ferromagnetic Cr(II) $S = 2$ ion.[22] Our instrumentation prevented us from measuring the hysteresis loop at $T = 2$ K, and so, it was not possible to estimate the canting angle for the system from the extrapolated value of $M_{nc}(T \rightarrow 0\ \text{K})$.[6d,23]

The hysteresis loop recorded at $T = 5.2$ K (see Figure 8a) shows again a nonlinear magnetic behavior, thus indicating that the compound is still in an ordered magnetic state. At $T = 6.0$ K, the M versus H plot is almost linear; therefore, at this temperature, the compound is in the paramagnetic state (see Figure 8b). The critical temperature can be then located at $T_N = 5.5$ K. The spin-canted ordered state is compatible with the crystal and molecular structure of the title compound because of the lack of the inversion center.[7] The phase change from paramagnetism to weak ferromagnetism seems to occur without an intermediate AF phase. This could be ascribed to the predominance of D, the single-ion anisotropy, over J/k, the exchange coupling (cf. with the small value of θ).

Conclusions

$Cr[(H_3N-(CH_2)_2-PO_3)(Cl)(H_2O)]$ was synthesized by reaction of $CrCl_2$ and 2-amino-ethyl-phosphonic acid in water in the presence of urea. Light-blue single crystals suitable for X-ray structure analysis have been isolated by precipitation from the same media. The Cr(II) ammonium−ethyl−phosphonate chloride represents an interesting example of a hybrid organic−inorganic material composed of mixed ionic and covalent layers. It shows a layered structure, made of inorganic and organic sheets alternating along the *b*-axis of the unit cell. The Cr(II) ions of the inorganic layer are pentacoordinated by four oxygen atoms, three oxygens coming from three different phosphonate ligands and one from the water molecule, and an fifth coordination site is occupied by an Cl^- anion in apical position giving rise to a square-pyramidal $[CrO_4 + 1Cl]$ chromophore. This kind of coordination is not very common in metal(II) phosphonates. The building up of this unusual network is driven by the formation of the organic ammonium group due to the acidic aqueous reaction medium and the presence of the Cl^- ions. Interestingly, the resulting intergrown structure is not centrosymmetric: the inorganic layers are interspersed by the ethylammonium groups attached to the phosphonic ligands, and the resulting crystal structure is polar. As far as we know, this is the first fully solved structure of a polar metal(II) phosphonate.[3] The protonation of the amino group has been confirmed by IR spectroscopy. $Cr[(H_3N-(CH_2)_2-PO_3)(Cl)(H_2O)]$ is paramagnetic down to 30 K, and it follows the Curie−Weiss law. The observed low negative value of the Weiss constant, $\theta = -2.2$ K, indicates a weak antiferromagnetic nearest-neighbor exchange coupling. A transition to a weak ferromagnetic state is observed at $T_N = 5.5$ K, and this is due to the spin-canting. In this situation, the local spins in the magnetic ordered state are not perfectly antiparallel, which results in an uncompensated moment in one direction. There are two known mechanisms originating a canted spin structure in these solids: (i) single-ion magnetic anisotropy[7b] and (ii) the so-called Dzyaloshinsky−Moriya exchange coupling, or antisymmetric exchange.[7c] In light of the structural and electronic properties of the compound, both the mechanisms could be responsible of the magnetic ordering. The phase change seems to occur without an intermediate long-range antiferromagnetic ordering state. This could be ascribed to the predominance of D, the single ion anisotropy, over J/k, the nearest-neighbor exchange coupling constant[7b,c] (cf. with the small negative value of θ). The weakness of the magnetic exchange can be rationalized by looking at the possible superexchange pathways existing in the lattice. Nearest neighbor Cr(II) ions are connected by

(22) Bellitto, C.; Staulo G. *J. Mater. Chem.* **1991**, *1*, 915.
(23) Palacio, F.; Antorrena, G.; Castro, M.; Burriel, R.; Rawson, J.; Smith, J. N. B.; Bricklebank, N.; Novoa, J.; Ritter, C. *Phys. Rev. Lett.* **1997**, *79*, 2336.

the phosphonic ligand, as Cr−O−P−O−Cr, and this pathway favors only weak antiferromagnetic interactions.

In conclusion, we have obtained a polar hybrid organic−inorganic material featuring a weak ferromagnetic state at low temperatures. It is now evident that the phenomenon of weak ferromagnetism is observed in molecule-based compounds with different metal ions and with a coordination around the metal ion other than six,[2,24] and in organic pure compounds.[23] An added value of this work is represented by the synthesis of a molecule-based compound which is polar and magnetic.[25]

Acknowledgment. This work was supported by the Consiglio Nazionale delle Ricerche (Italy). EU-COST D14 is also acknowledged for support. We thank also Dr. M. Green of the Royal Institution of Great Britain for magnetic measurements and Dr. A. Testa for helpful discussion and assistance.

Supporting Information Available: X-ray crystallographic file, in CIF format, for the structural determination of the title compound. This material is available free of charge via the Internet at http://pubs.acs.org.

IC0343197

(24) (a) Stock, N.; Frey, S. A.; Stucky, G. D.; Cheetham, A. K. *J. Chem. Soc., Dalton Trans.* **2000**, 4292. (b) Lumsden, M. D.; Sales, B. C.; Mandrus, D.; Nagler, S. E.; Thompson, J. R. *Phys. Rev. Lett.* **2001**, *86*, 159.

(25) Armentano, D.; DeMunno, G.; Lloret, F.; Palii, A. V.; Julve, M. *Inorg. Chem.* **2002**, *41*, 2007.